A RELATIVISTIC-PLASMA COMPTON MASER

JAMES C. WEATHERALL
Department of Physics, New Mexico Institute of Mining and Technology, Socorro, NM 87801

ABSTRACT

A relativistic pair-plasma that contains a high excitation of electrostatic turbulence could produce intense radiation by stimulated scattering at a brightness temperature in excess of 10^{20} K. Important relativistic effects would include the broadband frequency response of the plasma and Compton-boosting of the scattered radiation. In radio-frequency relativistic plasma, the optical depth can be as small as tens of meters. When the plasma wave excitation is one-dimensional and particle distributions have $T_\perp \ll T_\parallel$, the frequency-dependent angular distribution of the emission exhibits characteristics of pulsar emission.

Subject headings: instabilities — plasmas — pulsars: general — radiation mechanisms: nonthermal

1. INTRODUCTION

Radio emission at extremely high brightness temperature is possible from stimulated scattering in astrophysical plasmas with a high degree of plasma turbulence. Intensities on the order of 10^{20}–10^{30} K are suspected in some astrophysical objects, and an emission process of the form of a plasma maser may explain the extraordinary radio-frequency intensity of pulsars (Melrose 1996) and active galactic nuclei (Wagner & Witzel 1995). The calculation below exhibits the intensity and spectrum of emission in a relativistic plasma of electrons and positrons under the assumption of a uniform and high degree of excitation of plasma electrostatic wavemodes. It shows that the path length through the plasma can be relatively small for radiative growth, that Compton-like scattering increases the mean emission frequency above the plasma frequency, and that the frequency bandwidth of the emission is fairly narrow despite the broadband excitation in the plasma.

The calculation is done in a relativistic regime, since pair plasmas derive from extremely energetic processes, such as gamma-ray annihilation. Simulations of pair-plasma creation (Arendt & Eilek 2000) show that the pair-plasma distribution functions can be described by a thermal parameter that is moderately relativistic. In this paper, the kinetic temperature parameter $\rho = mc^2/(k_B T_K)$ is assigned a value of 1/10.

Conversion into electromagnetic modes by scattering off of plasma waves in nonrelativistic space plasma is known to produce radiation at the plasma frequency $\omega_p = (4\pi n e^2/m_e)^{1/2}$, and wave-wave coalescence at twice the plasma frequency (Gurnett et al. 1981). Radiation at these well-defined frequencies is due to the narrow frequency response in the plasma. It seems obvious that emission in a relativistic plasma is unlikely to follow this plasma-emission paradigm. For one thing, electrostatic modes in a relativistic plasma exist over a broad range of frequencies, $\omega_p \rho^{1/2} < \omega < \omega_p/\rho^{1/2}$ (Godfrey, Newberger, & Taggert 1975a, 1975b; Melrose et al. 1999). Furthermore, scattering by relativistic particles can modify frequencies by factors of $4\gamma^2$. Still, the stimulated emission appears to be fairly narrow in frequency, but this is a characteristic of maser emission due to frequency-dependent growth acting over many growth lengths.

Although this solution is illustrative of the relativistic effects in plasma emission, several assumptions are used to simplify the calculation. First, the excitation of the turbulence is characterized by a single temperature parameter, without regard for specific plasma-streaming or shock-excitation mechanisms, or wave cascades. For example, in thermal equilibrium, the energy density in plasma waves relative to the kinetic energy density, $E^2/(8\pi n k_B T_B)$, is inversely proportional to the number of particles in a Debye cube, $n\lambda_D^3 = n[c/(\omega_p \rho^{1/2})]^3$. This parameter can be quite large for astrophysical plasmas. If a radio-frequency plasma ($\nu_p \sim 3$ GHz) manages an equipartition between turbulent electrostatic energy and thermal kinetic energy at temperatures of $T_K \sim 5 \times 10^{10}$ K, the characteristic excitation as described by an enhanced nonlinear temperature $T_{NL} = (n\lambda_D^3)T_K$ could be more than 10^{22} K. This coherent enhancement of scattering off of plasma waves was recognized by Gailaitis & Tsytovich (1964), and Colgate, Lee, & Rosenbluth (1970).

Another simplification is to do the calculation without an imposed background magnetic field. This justifies the assumption of isotropy in the particle distributions, wave spectra, and wave dispersion. Including a magnetic field would tend to make the turbulence one-dimensional in the direction of the magnetic field, and would modify the dispersion properties of the electromagnetic modes. Thus, the plasma maser in a magnetized plasma would not be isotropic in direction, but would have preferred directions for emission. The effect of making the maser plasma one-dimensional is illustrated by an example.

Finally, the turbulent excitation is assumed to be steady. This energy reservoir of turbulence must be maintained against radiation loss by an injection process, but to model this requires an additional kinetic model for the turbulence. The assumption of constant wave excitation can be expected to fail when the brightness temperature greatly exceeds the wave temperature and radiation becomes a significant energy sink. Radiative losses will also determine the lifetime of the system.

The calculation proceeds from classical scattering rates between plasma and electromagnetic wave modes. The kinetic equation is put into the form of a radiative transfer equation in the next section, assuming a kinetic temperature for the plasma and a nonlinear effective temperature for the plasma turbulence. The necessary integrals for the scattering coefficients are done numerically, as described in § 3.

The intense emission that can derive from the maser process is discussed in § 4.

2. TRANSFER EQUATION

We start with a transfer equation between the plasma waves and electromagnetic radiation (see, for example, Melrose 1980, § 5.4). For this equation, the electromagnetic wave spectrum is described by the photon number density function, $N_T(k)$, and the plasma wave spectrum is described by the number density function $N_L(k)$. (The number density spectrum is also called the occupation number.) The subscripts T and L denote "transverse" and "longitudinal."

By definition, the number of photons with wavevector k in a phase space volume d^3k around k is given by $N(k)[d^3k/(2\pi)^3]$. The integral of $N(k)$ over phase space will give the number of photons per cm^3.

The plasmon occupation number can be formulated from the electric field energy spectrum of the turbulent waves,

$$W = \frac{1}{VT} \int \frac{E(r, t)E(r, t)}{4\pi} dV \, dt$$
$$= \frac{1}{VT} \int \frac{d^3k}{(2\pi)^3} \frac{d\omega}{2\pi} \frac{E^*(k, \omega)E(k, \omega)}{4\pi} , \quad (1)$$

averaged over time T and volume V. Assuming well-defined wavemodes, $E(k, \omega) = E(k)2\pi\delta(\omega - \omega_L(k))$, the integration over ω gives

$$W = \int \left[\frac{1}{V} \frac{E^*(k)E(k)}{4\pi} \right] \left[\frac{d^3k}{(2\pi)^3} \right] . \quad (2)$$

Because the term in second brackets is the number density of wavemodes between k and $k + dk$, it is easy to identify the first term in brackets as the electrostatic energy per wavemode. We apply a thermal-like excitation of normal modes in the turbulence to derive

$$\frac{1}{V} \frac{E^*(k)E(k)}{4\pi} = \frac{1}{2} k_B T_{NL} . \quad (3)$$

For electrostatic waves, another degree of freedom is invested in the particle motion. Finally, the occupation number is acquired from a semiclassical formula,

$$N_L(k) = \begin{cases} k_B T_{NL}/\hbar\omega_L(k) & \sqrt{\rho}\omega_p < kc < \omega_p/\sqrt{\rho} , \\ 0 & \text{otherwise .} \end{cases} \quad (4)$$

The inequality describes the frequency range of plasma normal modes in a relativistic plasma.

With this notation, the transfer equation in the classical limit for photons in plasma turbulence is given by (Melrose 1980, eq. [5.89])

$$\frac{dN_T(k)}{dt} = \int \frac{d^3k'}{(2\pi)^3} d^3p \, n\varpi_{TL}(p, k, k')$$
$$\times \left\{ f(p)[N_L(k') - N_T(k)] \right.$$
$$\left. + N_L(k')N_T(k)\hbar(k - k') \cdot \frac{\partial f}{\partial p} \right\} . \quad (5)$$

The longitudinal-to-transverse scattering probability is denoted by ϖ_{TL} (see eq. [16]). The three-dimensional thermal distribution of lepton momentum in a relativistic plasma is given by the normalized function $f(p) \, d^3p = \{\exp[-\rho\gamma(p)]/Z\} \, d^3p$, where $Z = [4\pi K_2(\rho)]/\rho$, K_2 is the modified Bessel function, $\gamma = [1 + p^2/(m^2c^2)]^{1/2}$, and ρ is the temperature parameter. The spatially averaged number density of particles in the zero-momentum reference frame is n. To write this equation in terms of the specific intensity $I(\omega)$ for a single polarization, we use

$$I(\omega) \, d\omega \, d\Omega = \hbar\omega N_T(\omega/c)c \frac{k^2 \, dk \, d\Omega}{(2\pi)^3} . \quad (6)$$

The resulting equation for the change in intensity over path length, $ds = c \, dt$, has three terms. The first term represents spontaneous scattering,

$$\frac{dI}{ds} = \Lambda_1(\omega) \frac{\omega^2}{(2\pi)^3c^3} k_B T_{NL} , \quad (7)$$

where the emission coefficient has been put into the form

$$\Lambda_1(\omega) = \int \frac{d^3k'}{(2\pi)^3} nf(p) \, d^3p \, \varpi_{TL}(p, k, k') \frac{\omega}{\omega'} , \quad (8)$$

where $\omega' = \omega_L(k')$, and $\omega = \omega_T(k)$. The second term represents absorption,

$$c \frac{dI}{ds} = -\Lambda_2(\omega)I(\omega) , \quad (9)$$

where the absorption coefficient is

$$\Lambda_2(\omega) = \int \frac{d^3k'}{(2\pi)^3} nf(p) \, d^3p \, \varpi_{TL}(p, k, k') . \quad (10)$$

The final term contributes to stimulated scattering. For a thermal distribution, the momentum derivative gives

$$\frac{\partial f}{\partial p} = -\frac{cf(p)}{k_B T} \beta . \quad (11)$$

The vector arithmetic can be worked out using the kinematic relationship between frequencies,

$$\omega' = \omega \frac{1 - \beta \cos \theta}{1 - \beta \cos \theta'} , \quad (12)$$

where the angles are between the wavevectors and the electron velocity vector. Thus,

$$\hbar(k - k') \cdot \frac{\partial f}{\partial p} = -\frac{\hbar\omega}{k_B T} \left(1 - \frac{\omega'}{\omega}\right)f(p) . \quad (13)$$

The stimulated scattering term is

$$c \frac{dI}{ds} = \frac{T_{NL}}{T} [\Lambda_2(\omega) - \Lambda_1(\omega)]I(\omega) . \quad (14)$$

The complete transfer equation is

$$\frac{dI(\omega)}{ds} = \Lambda_1 \frac{\omega^2 k_B T_{NL}}{(2\pi)^3c^3} + \left[-\Lambda_2 + \frac{T_{NL}}{T}(\Lambda_2 - \Lambda_1)\right] \frac{I(\omega)}{c} . \quad (15)$$

3. FORMULATION OF THE SCATTERING COEFFICIENTS

The probability for the scattering of longitudinal waves into transverse waves by relativistic electrons is given by
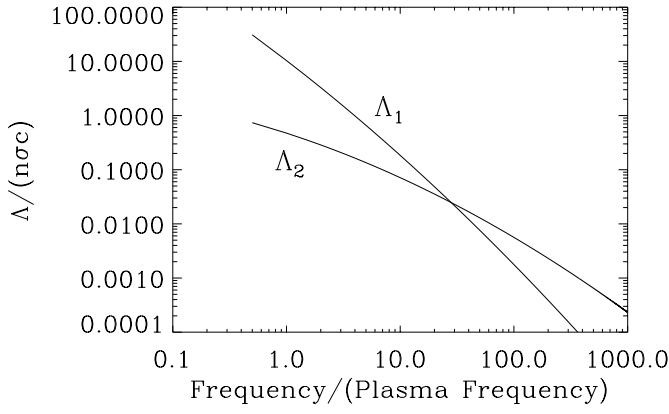
Fig. 1.—Scattering coefficients determined numerically from equations (18) and (22) for isotropic thermal particles of temperature $k_B T_K = 10mc^2$.

(Melrose 1980 eq. [4.150], 1971)

$$n\varpi_{TL}(p, k, k') \frac{d^3k'}{(2\pi)^3} = \frac{(2\pi)^3 ne^4}{m^2\omega'\omega} \frac{(1 - \beta^2)}{(1 - \hat{k}\cdot\beta)^2(1 - \hat{k}'\cdot\beta)^2}$$

$$\times \delta(\omega(1 - \hat{k}\cdot\beta) - \omega'(1 - \hat{k}'\cdot\beta))$$

$$\times \left\{ (1 - \hat{k}\cdot\beta)^2[1 - (\hat{k}'\cdot\beta)^2] \right.$$

$$\left. - (1 - \beta^2)(\hat{k}\cdot\hat{k}' - \hat{k}'\cdot\beta)^2 \right\} \frac{d^3k'}{(2\pi)^3}, \quad (16)$$

where use is made of $\omega' = k'c$ for the relativistic plasma mode. The term $n\varpi_{TL}(p, k, k') d^3k'$ has units of s^{-1}. In equation (16), a sum is made over polarization in the scattered waves.

The integration of the scattering rates over d^3k' and d^3p is done in spherical coordinates, in which the angle θ' measures k' relative to β and θ measures β relative to k. In terms of angle cosines $\mu = \cos\theta$,

$$d^3k' = \frac{\omega'^2}{c^3} d\omega' d\phi' d\mu',$$

$$d^3p = p^2 dp d\phi d\mu. \quad (17)$$

The integral over $d\omega'$ can be done easily with the delta function. After integration over $d\phi'$ and $d\phi$, the remaining integrals over angle in the emission rate are

$$\Lambda_1(\omega) = \frac{3}{16} n\sigma_T c$$

$$\times \int 4\pi p^2 f(p) dp \int_{\mu_{min}}^{1} \frac{1 - \beta^2}{1 - \beta\mu} d\mu$$

$$\times \int_{-1}^{\mu'_{max}} \frac{A + B\mu'^2}{(1 - \beta\mu')^4} d\mu', \quad (18)$$

where A and B are algebraic functions of μ,

$$A = 1 + \beta^2 - 4\beta\mu + \mu^2 + \beta^2\mu^2,$$

$$B = 1 - 5\beta^2 + 2\beta^4 + 4\beta\mu - 3\mu^2$$

$$+ 3\beta^2\mu^2 - 2\beta^4\mu^2. \quad (19)$$

The upper cutoff to the $d\mu'$ integral is a by-product of the delta function and the high-frequency bound on $\omega' < (1 + \beta)\gamma\omega_p$. Thus,

$$\mu'_{max} = \min\left\{\frac{1}{\beta} - \frac{\omega(1 - \beta\mu)}{2\beta\gamma\omega_p}, 1\right\}. \quad (20)$$

In order for μ'_{max} to be larger than -1, the angles μ must be larger than

$$\mu_{min} = \max\left\{\frac{1}{\beta} - \frac{1 + \beta}{\beta} \frac{2\gamma\omega_p}{\omega}, -1\right\}. \quad (21)$$

Similarly, the absorption rate

$$\Lambda_2(\omega) = \frac{3}{16} n\sigma_T c \int 4\pi p^2 f(p) dp$$

$$\times \int_{\mu_{min}}^{1} \frac{1 - \beta^2}{(1 - \beta\mu)^2} d\mu \int_{-1}^{\mu'_{max}} \frac{A + B\mu'^2}{(1 - \beta\mu')^3} d\mu'. \quad (22)$$

The integrals in the above equation are completed numerically. Solutions for $\Lambda_1(\omega)$ and $\Lambda_2(\omega)$ are shown in Figure 1. The two scattering rates are equal ($\Lambda_1 \sim \Lambda_2$) near the characteristic frequency $\omega_p(1/\rho^{3/2})$.

4. AMPLIFICATION BY STIMULATED EMISSION

With fixed values for the wave temperature T_{NL} and the kinetic temperature T_K, the transfer equation is a first-order differential equation with constant coefficients, which can be solved directly as a function of path length:

$$I = I_K e^{s\Lambda_{stim}/c} + I_{NL} \frac{\Lambda_1}{\Lambda_{stim}} (e^{s\Lambda_{stim}/c} - 1), \quad (23)$$

where the effective stimulated scattering rate is

$$\Lambda_{stim}(\omega) = (\Lambda_2 - \Lambda_1)T_{NL}/T_K - \Lambda_2. \quad (24)$$

At low frequency ($\omega \ll \omega_p \rho^{-3/2}$), $\Lambda_1 \gg \Lambda_2$, and the intensity is limited to the kinetic temperature. Near the characteristic frequency, the intensity saturates at the nonlinear wave temperature. At higher frequencies, the intensity increases exponentially. However, the exponentiation rate diminishes at frequencies much higher than the characteristic frequency, since Λ_1 and Λ_2 become small.

The high brightness temperatures derived from this theory must be qualified by the fact that cooling of the plasma and turbulence are not taken into account. A full picture of the energy balance requires additional kinetic equations for the plasma waves and particle energy distribution. However, it is easy to estimate how long the plasma can maintain its relativistic energy against Compton loss. At 10^{22} K, a 10^3 cm scale system (such as a pulsar magnetospheric source region) will last 10^{-6} s, and a 10^{14} cm scale system (encompassing an active galactic nucleus accretion region) will last for 10^5 s against radiative loss. These simple numbers suggest how maser lifetime might relate to microstructure in pulsar radio emission and intraday variability in quasi-stellar objects (QSOs).

To show the magnitude of stimulated emission, the scattering coefficients can be scaled as

$$\frac{s\Lambda}{c} \frac{T_{NL}}{T_K} = 1.3 \times 10^{-10} \frac{T_{NL}}{T_K} \left(\frac{\Lambda}{n\sigma_T c}\right)$$

$$\times \left(\frac{n}{10^{11} \text{ cm}^{-3}}\right)\left(\frac{s}{1000 \text{ cm}}\right). \quad (25)$$

Substantial growth in intensity occurs in path lengths smaller than a kilometer, assuming turbulence temperatures of $T_{\rm NL}/T_K \geq 10^{12}$, as demonstrated in Figure 2. Such a large temperature for the turbulence is not implausible from an energy standpoint. The turbulent temperature estimated from equipartition between electrostatic and plasma kinetic energy is

$$\frac{T_{\rm NL}}{T_K} \sim \left(\frac{c^3\sqrt{n}}{\omega_p\sqrt{\rho}}\right)^3 = 6 \times 10^{13}\left(\frac{10^{11}\ {\rm cm}^{-3}}{n}\right)^{1/2}\left(\frac{0.1}{\rho}\right)^{3/2} \ . \tag{26}$$

For a plasma kinetic temperature on the order of 10^{10} K, radiative brightness temperatures greater than 10^{23} K are consistent with stimulated emission from this mechanism. Higher brightness temperatures are possible with greater turbulent temperature or larger path lengths, depending on the limits that are imposed by Compton cooling.

In summary, the relativistic-plasma Compton maser uses free energy in the form of wave turbulence to produce electromagnetic radiation via induced scattering in the relativistic thermal plasma. The high brightness temperature derives from the large value of the plasma parameter, $n[c/(\omega_p \rho^{1/2})]^3$, which is generally true in astrophysical plasmas, although less so in laboratory plasmas. The maser turbulence conversion mechanism is an alternative to other plasma turbulence conversion processes invoking coherent spatial effects or nonlinear wave dynamics (for example, Weatherall 1997, 1998; Asseo, Pelletier, & Sol 1990), which may not develop because of the turbulence being strongly driven or highly inhomogeneous.

The turbulent conversion process described here might also apply to pulsars. Maser models are not new to pulsar radiation physics (for example, Lyutikov, Machabili, & Blandford 1999; Luo & Melrose 1995), but these masers resemble free-electron masers in which particle beams generate the emission. A model invoking the Compton plasma maser requires further inclusion of anisotropies due to the magnetic field, wave-dispersion properties in magnetized plasma, and specific mechanisms for wave excitation by collimated particle beams. However, we can simulate these effects by limiting the plasma momentum distribution and turbulent wavevectors to a single coordinate axis.
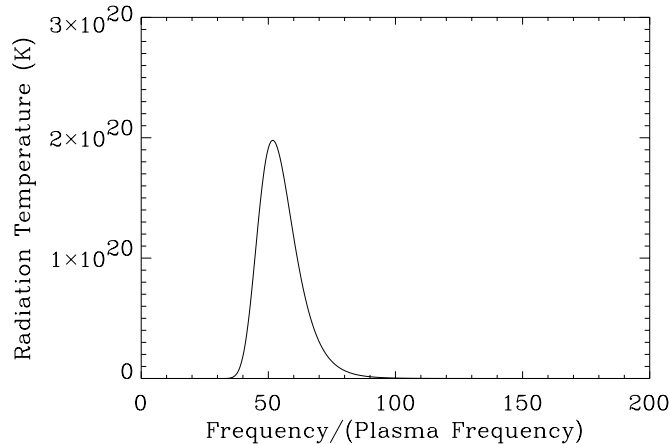

FIG. 2.—Intensity of plasma maser emission in an electron-positron plasma, with a kinetic temperature of $10mc^2$. The turbulent excitation is taken to be enhanced by $T_{\rm NL}/T_K = 10^{12}$. Scaling to a plasma frequency of $f_0 = 3$ GHz, the path length corresponds to $s = 2 \times 10^5$ cm.
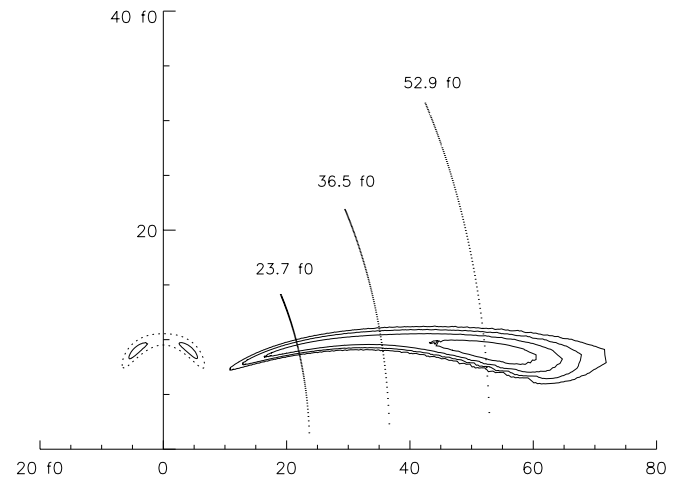

FIG. 3.—Contours of constant brightness temperature in frequency space for the Compton maser for one-dimensional turbulence with $T_{\rm NL}/T_K = 10^{12}$, and a path length of $s = 1.5 \times 10^6$ cm. The frequency is in units of the plasma frequency, f_0. The contour levels are 1, 2, 4, and 8×10^{16} K. The contours for both the plasma rest frame and the lab frame in which the plasma moves with $\gamma = 3.8$ are shown: the lowest contour is dotted in the former case. Intensity along the three cuts of constant frequency are presented in the next figure.

In one dimension, the differential scattering cross sections in terms of the angle cosine μ between the emission wave-vector $\boldsymbol{k}$ and the z-coordinate axis are given by

$$\frac{d\Lambda_2(k,\mu)}{d\Omega} = \int \frac{dk'}{(2\pi)^3}\frac{\omega'^2}{c^2}\int n\,dp f(p)\varpi_{\rm TL}(p,k',\boldsymbol{k}) \ ,$$

$$\frac{d\Lambda_1(k,\mu)}{d\Omega} = \int \frac{dk'}{(2\pi)^3}\frac{\omega'^2}{c^2}\int n\,dp f(p)$$
$$\times \left(\frac{1\pm\beta}{1-\beta\mu}\right)\varpi_{\rm TL}(p,k',\boldsymbol{k}) \ . \tag{27}$$

The choice of sign is "$+$" for electrostatic waves with k' in the *negative* z-direction, and "$-$" for waves in the *positive* z-direction. The calculation assumes that waves have a relativistic dispersion relation $\omega' = k'c$ and that the uniform excitation applies to frequencies $\omega_p \rho^{1/2} < \omega' < \omega_p/\rho^{1/2}$. The one-dimensional electron distribution function is given by $f(p)\,dp = \exp\left[-\rho\gamma(p)\right]dp/[2K_1(\rho)]$, where K_1 is the modified Bessel function.

The transfer equation is the same as before, substituting for the scattering rates: $\Lambda_1 \to \Delta\Omega(d\Lambda_1/d\Omega)$ and $\Lambda_2 \to \Delta\Omega(d\Lambda_2/d\Omega)$. Here $\Delta\Omega$ is the range of solid angles about the turbulence axis that have nonlinear excitation. The important difference in one dimension is the directivity of the maser. Figure 3 is a polar plot in angle and frequency. The emissivity in the plasma rest frame is largest in the directions *near* perpendicular to the magnetic axis, with some angular structure due to relativistic thermal velocities. However, the plasma is moving relative to the lab/star frame because of the polar cap current flow, and the emission can be expected to be beamed relativistically: this is illustrated in the figure with a Lorentz transformation.

One intriguing consequence of the moving maser is the angular dependence of the peak emission for different frequencies. Radio pulsars show a variation in pulse profile (intensity versus phase) for different observing frequencies. This is generally interpreted as radius-to-frequency
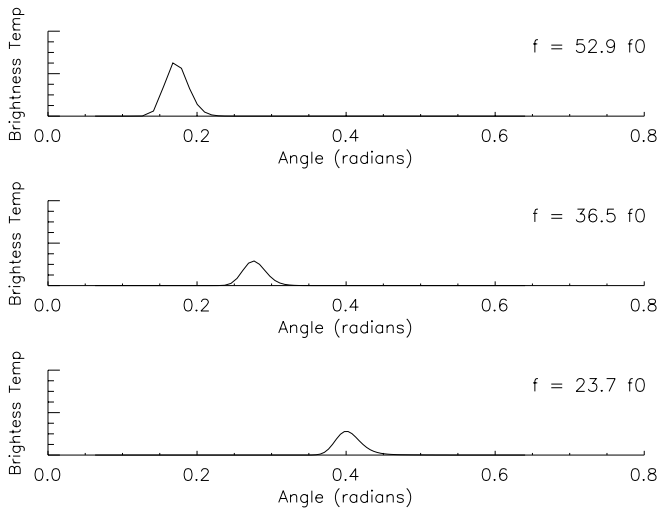
FIG. 4.—Brightness temperature vs. angle for three different frequencies, for the case of a moving plasma. The temperature scale is the same for each plot, with a scale maximum at 1.5×10^{17} K.

mapping, based on the presumption that the emission comes from different heights in the polar cap, and that the emission frequency is tied to the local plasma frequency. As is clearly shown in Figure 4, the maser emission from a single location can produce similar frequency-dependent profiles.

Finally, we remark that relativistic temperatures have the effect of supporting wave frequencies that are in a broad range about the plasma frequency: still, the highest growth occurs at frequencies above the plasma frequency. Thus, relativistic effects do not appear to mitigate the puzzle that emission at the local plasma frequency in the pulsar polar-cap plasma produces frequencies that seem high for radio emission (Melrose & Gedalin 1999; Kunzl et al. 1998).

REFERENCES

Arendt, P., & Eilek, J. A. 2000, in IAU Colloq. 177, Pulsar Astronomy—2000 and Beyond, ed. M. Kramer, N. Wex, & N. Wielebinski (ASP Conf. Ser. 222; San Francisco: ASP), 445
Asseo, E., Pelletier, G., & Sol, H. 1990, MNRAS, 247, 529
Colgate, S. A., Lee, E. P., & Rosenbluth, M. N. 1970, ApJ, 162, 649
Gailaitis, A., & Tsytovich, V. N. 1964, Soviet Phys. JETP Lett., 19, 1164
Godfrey, B. B., Newberger, B. S., & Taggert, K. 1975a, IEEE Trans. on Plasma Sci., PS-3, 60
———. 1975b, IEEE Trans. on Plasma Sci., PS-3, 68
Gurnett, D. A., Maggs, J. E., Gallagher, D. L., Kurth, W. S., & Scarf, F. L. 1981, J. Geophys. Res., 86, 8833
Kunzl, T., Lesch, H., Jessner, A., & von Hoensbroech, A. 1998, ApJ, 505, L139

Luo, Q., & Melrose, D. B. 1995, MNRAS, 276, 372
Lyutikov, M., Machabili, G. Z., & Blandford, R. D. 1999, ApJ, 512, 804
Melrose, D. B. 1971, Ap&SS, 10, 197
———. 1980, Plasma Astrophysics, Vol. 1 (New York: Gordon and Breach)
———. 1996, in IAU Colloq. 160, Pulsars: Problems and Progress, ed. S. Johnston, M. A. Walker, & M. Bailes (San Francisco: ASP), 139
Melrose, D. B., & Gedalin, M. E. 1999, ApJ, 521, 351
Melrose, D. B., Gedalin, M. E., Kennett, M. P., & Fletcher, C. S. 1999, J. Plasma Phys., 62, 233
Wagner, S. J., & Witzel, A. 1995, ARA&A, 33, 163
Weatherall, J. C. 1997, ApJ, 483, 402
———. 1998, ApJ, 506, 341